


 Cite this: *RSC Adv.*, 2022, **12**, 33264

Dicationic amphiphiles bearing an amino acid head group with a long-chain hydrophobic tail for *in vitro* gene delivery applications†

 Shreesha Manturthi,^a Kumar Pranav Narayan^{*b} and Srilakshmi V. Patri^{†,a}

Amino acid-based cationic lipids, which have proven their efficacy as plasmid DNA nanocarriers, were employed as dicationic forms to transfect genes into cancer and non-cancer cells in this study. Proline, methionine, and serine amino acids are involved as hydrophilic moieties and the hydrocarbon long-chain serves as a hydrophobic tail. In a multicultural investigation, cationic lipids were employed as nanovectors in conjunction with the helper lipid DOPE. To quantify the lipid efficient size, charge, and pDNA binding, biophysical analyses such as hydrodynamic diameter, zeta potential, agarose gel electrophoresis, and serum stability were done primarily. The liposomal particle composition was examined by scanning electron microscopy (SEM). Synthesized dicationic vector lipoplex formulations with reporter genes were found to be non-toxic to the cells investigated by MTT assay, and in addition, therapeutic gene p53 transfected into oral and brain cancer cells causing cell death was examined. *In vitro* investigations further validated that the proline-based lipid (C14-P) has high gene knockdown efficacy than methionine-based lipid (C14-M) and serine-based lipid (C14-S) at optimal N/P ratios as measured by β -galactosidase protein and eGFP expression. C14-P lipid shows superior cellular internalization compared to C14-M and C14-S in HEK-293 and CAL-27 cells attested by confocal study. These findings could include the proline-based lipid vector's exceptional gene delivery activity.

Received 21st September 2022
 Accepted 28th October 2022

DOI: 10.1039/d2ra05959b
rsc.li/rsc-advances

1. Introduction

The development of secure and reliable therapeutic gene carriers is still a major problem in gene therapy, which is used to treat a wide range of hereditary illnesses, deadly viral diseases, and malignancies. The two types of gene delivery agents generally in use are viral and non-viral. Despite their remarkable efficiency, recombinant viral vectors have a number of biodefense issues.^{1–3} Viral vectors can generate erythrogenic and biocompatible reactions to their internal system and produce conceivably clone-competent viruses *via* related species with the host genetic material.^{4,5} Moreover, the therapeutic genes that could be placed inside viral vectors get a small insertion size constraint. As a result, a rising number of studies are being published on the creation of non-viral competitors such as cationic amphiphiles, also referred to as cationic transfection lipids,^{6–8} cationic polymers,⁹ dendrimers,¹⁰ and

other non-viral alternatives. Cationic amphiphiles are rising in popularity as innovative non-viral transfection carriers of preference for transporting genes into the human body cells because of their low immunogenicity, durable manufacturing, ability to transfer large chunks of pDNA, and flexibility of dealing and preparation processes.^{11–15} The biomolecular frameworks of cationic amphiphiles are made up of a polar head group, which is a positively ionised hydrophilic region and a hydrophobic body, which is a nonpolar region (usually consisting of vitamin-E or a cholesterol skeleton or long aliphatic hydrocarbon chains *etc.*) often fasten conjugation through a linker feature such as amide, amidine, ether, ester, *etc.* The strategy of intracellular delivery of plasmid DNA to the cytoplasm or nucleus has been investigated using several cationic liposomes to improve gene expression efficacy.^{16,17} Membrane merging happens between the cationic lipid portion and the membrane of early endosomes (pH 6.0–6.5), whenever lipoplexes are taken hold by the selected cell, resulting in the release of nucleic acids into the cytoplasm. Generally delivered nucleic acids assemble in the nucleus.¹⁸ Mostly, hydrophilic domains are generated from amino acids,^{19–21} heterocyclic moieties,^{7,22} sugar moieties,^{23,24} *etc.*, and have been contributing propensity in cancer gene therapy. For decades, long aliphatic hydrocarbon chains have been handled as a hydrophobic tail in gene delivery to several cancer cells by its particular aspect in easily forming liposomal vesicles.^{25–27}

^aDepartment of Chemistry, National Institute of Technology Warangal, Hanamkonda, Telangana-506004, India. E-mail: patrisrilakshmi@nitwc.ac.in

^bDepartment of Biological Science, Bits Pilani-Hyderabad, Hyderabad, Telangana-500078, India. E-mail: pranav@hyderabad.bits-pilani.ac.in

† Electronic supplementary information (ESI) available: Experimental procedure, ¹H-NMR, ¹³C-NMR, ESI-HRMS spectra, and HPLC chromatogram purity of compounds are provided. EGFP qualitative and quantitative analysis in U87 cells and cellular uptake qualitative and quantitative analysis in HEK-293 cells are provided. See DOI: <https://doi.org/10.1039/d2ra05959b>



Proline (Pro) is the only amino acid containing a ring structure having a secondary α -amino group, and this structural trait affords gene carriers containing the proline group distinct specific chemical and biological features. Hydrolysable proline-rich sequences have been identified as natural sources of cell-permeant vectors that can crack the phospholipid bilayer and transport the associated payloads without inflicting baleful membrane rupture.^{21,28,29} Serine (Ser) is a natural amino acid that contains a hydroxy functional group, which has been used in *in vitro* gene delivery as a hydrophilic moiety and shows its optimal transfection results in multiple cancerous cells.^{25,30} On multiple levels, methionine (Met) metabolism has been linked to cancer. Although they can rapidly manufacture methionine from homocysteine, many cancer cells cannot multiply in a media wherein methionine is substituted by homocysteine.^{31,32} When methionine is used as a hydrophilic moiety in cationic lipids, its metabolic character may impact gene delivery. Proline, serine, and methionine amino acids having important functional aspects are cyclic amine, hydroxy group, and sulphur group, respectively, which strongly influence gene carrying and delivery by their low toxicity and high biodegradability.

These notable properties of proline, serine, and methionine inspired us to develop lipids with these amino acids in the head group region. Three dicationic lipids, namely **C14-P**, **C14-M**, and **C14-S**, were prepared, carrying the hydrophobic fourteen carbons di long-chain moiety, applied as gene delivery vectors in this work. As part of gene delivery, synthesized vectors could deliver reporter genes as well as therapeutic genes. A tumor-suppressor gene with a well-defined function is the p53 gene. In 1991, the first proof that p53 can trigger apoptosis was reported.^{33,34} Since a great deal of attention has been paid to the cellular basis that p53 triggers cells to produce apoptosis.³⁵ In this study, synthesized vectors delivering the p53 gene that causes cancer cell apoptosis is reported.

2. Results and discussion

2.1. Chemistry

The major hydrophobic elements common to all the three lipids **C14-P** (**L1**), **C14-M** (**L2**), and **C14-S** (**L3**) (Fig. 1) outlined herein are (i) 14 carbon di long-chain as an anchoring group prevalent in all three lipids, (ii) differing hydrophilic groups with three amino acids, and synthetic procedure of dicationic lipids, as shown in Scheme 1. The chemistry required to build these dicationic lipids is as follows. First, the tertiary amine having two hydrophobic long-chain $(\text{C14})_2\text{NEOH}$ (2-(ditetradecylamino) ethanol) is generated by *N*-alkylation of ethanolamine using 1-bromo tetradecane reacting with ethanolamine in the presence of potassium carbonate (K_2CO_3). Then, 2-(ditetradecylamino) ethanol is coupled with Fmoc-amino acid using coupling reagents *p*-toluene sulfonic acid (PTSA), dicyclohexylcarbodiimide (DCC), and base 4-dimethylaminopyridine (DMAP) derived tertiary amine coupled Fmoc-amino acids (**1a**, **2a**, and **3a**). This is followed by deprotection of the Fmoc group deprotected with piperidine in the presence of DMF and then quaternization using HCl to yield **C14-P**, **C14-M**, and **C14-S** dicationic lipids. $^1\text{H-NMR}$, $^{13}\text{C-NMR}$, and ESI/

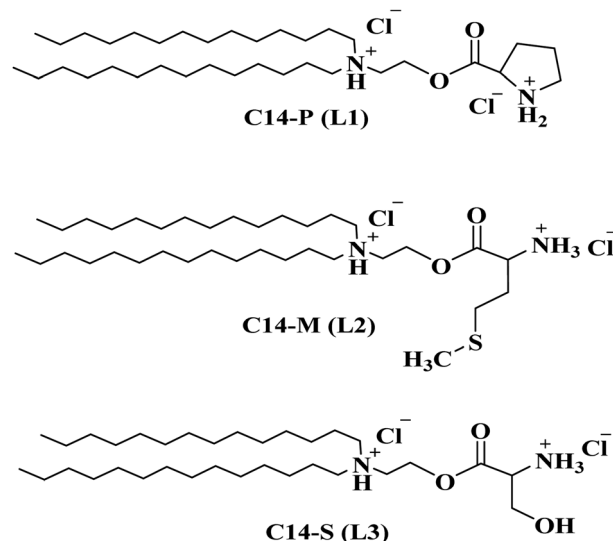


Fig. 1 Chemical composition of synthesized dicationic lipids.

HRMS mass spectra validated the chemical structures of all the synthetic intermediates and final amphiphiles represented in ESI (Fig. S1–S21†). HPLC analytical chromatogram was used to detect the purity of the final lipids, as described in Fig. S22–S24.† The mobile phase was a mixture of methanol (65%) and water (35%), which are HPLC grade and the stationary phase was a porous graphitic carbon column for the sample run. The lipid (1 mg) was dissolved in 1 mL of methanol solvent and 20 μL of the sample was injected for analysis at 15 min time point. The purity of peaks that appeared at retention times were 8.50, 8.13, and 7.15 for **C14-P**, **C14-M**, and **C14-S**, respectively. All three lipids were analysed as pure, above 90%.

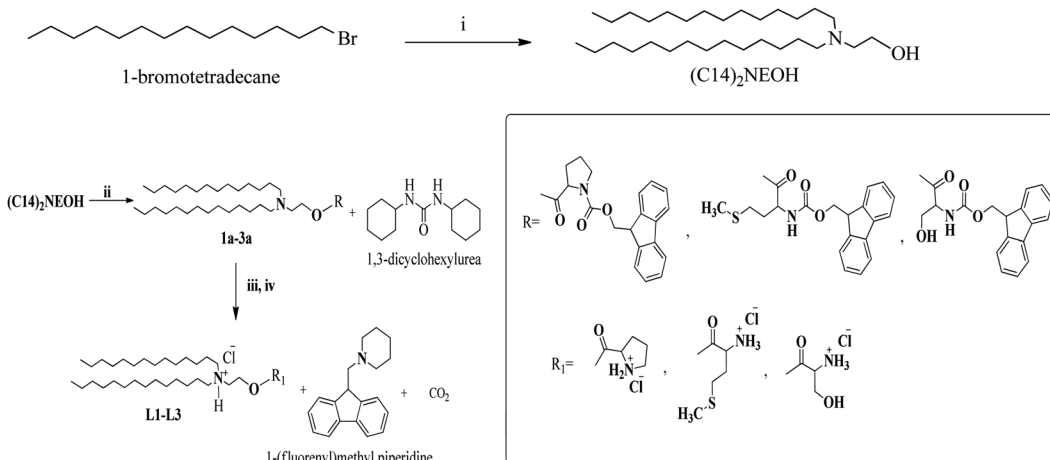
2.2. Small uni-lamellar vesicles (SUVs)

Many previous non-viral vector installations demonstrated that merged liposomal formulations (lipid : co-lipid) might have improved transfection potentials than simple cationic formulations (lipid alone).^{36,37} DOPE is a zwitter ionic phospholipid that has been widely employed as a helper lipid in many research studies due to its fusogenic nature and non-bilayer structure development, which aids in the disruption of the endosomal barrier after intracellular uptake of liposome into the cytoplasm.³⁸ Initially, we attempted to create lipid : DOPE (liposome) vesicles by mixing DOPE with cationic lipids (**C14-P**, **C14-M**, and **C14-S**) in various molar combinations, but the suspensions were neither transparent nor successful in transfection. We stepped up our attempts to discover a better formulation with DOPE to achieve the plasmid delivery properties of these lipid derivatives. Clear and uniform lipid : co-lipid formulations were achieved at a 1 : 1 molar ratio without any suspension and were stable at 4 °C for up to 10 weeks.

2.3. Physico-chemical properties of **C14-P**, **C14-M**, and **C14-S** liposomes and their lipoplexes

The physico-chemical properties of cationic lipids play a vital role in achieving effective transfection. The diameter of the





Scheme 1 Synthetic path to L1, L2, and L3: reagents and conditions: (i) ethanolamine, potassium carbonate (K_2CO_3), ethyl acetate, reflux $60\text{ }^\circ\text{C}$, 12 h. (ii) Fmoc-proline/Fmoc-methionine/Fmoc-serine, *p*-toluene sulfonic acid (PTSA), 4-dimethylaminopyridine (DMAP), dicyclohexylcarbodiimide (DCC), dichloromethane (DCM), RT, overnight. (iii) Piperidine, dimethylformamide (DMF), RT. (iv) 6 N HCl, reflux, 12 h.

lipoplex, the proportion of lipids to plasmid DNA, morphology of the liposome, and the composition of the liposome are all important aspects of cellular nucleic acid transport. The physico-chemical features of liposomes that have been complexed with nucleic acids may differ from those of regular liposomes. The analysis was performed using dynamic light scattering (DLS) with liposomes (lipid : DOPE-1 : 1) and complexes (lipid : pDNA) at various N/P ratios of 1 : 1, 2 : 1, 4 : 1, and 8 : 1. The sizes of **C14-P**, **C14-M**, and **C14-S** liposomes were revealed to be 149 nm, 123 nm, and 122 nm, respectively, as shown in Fig. 2A. The sizes of the lipoplexes were observed increase dramatically from 164 nm to 384 nm, 131 nm to 358 nm, and 125 nm to 344 nm as the N/P ratio of lipid : pDNA complexes of **C14-P**, **C14-M**, and **C14-S** was extended from 1 : 1 to 8 : 1, respectively (Fig. 2C). The rise in the size with increasing N/P ratio could be explained by better subspaces at higher lipid contents. Furthermore, the maximum range of the size of the lipoplexes is 384 nm, demonstrating that they will be regarded to be optimal for effective gene transfections. The dicationic liposomes of **C14-P**, **C14-M**, and **C14-S** surface charges are +67, +73, and +74 mV, respectively (Fig. 2B). The surface potential of lipoplexes decreased compared to the corresponding liposomes when neutralized with pDNA (Fig. 2D). According to these findings, the proper size and surface potential of lipoplexes are necessary for successful transfection. Scanning electron microscopy was utilized to pictorially assess the DLS findings regarding the liposomal compositions. The visual images in Fig. 2E show that the liposomal particle sizes are substantially identical to the DLS results.

2.4. Interaction of liposomes with pDNA, heparin displacement and serum stability

Gel electrophoretic assay is used to analyse the ionic interactions between the nucleic acid and the current lipids **C14-P**, **C14-M**, and **C14-S** as a function of lipid : pDNA N/P ratio. For pDNA binding experiments, liposomal formulations of 1 : 1 (lipid : DOPE) molar ratio were utilized. The results of this gel electrophoresis analysis demonstrated that lipids had strong

lipoplex, the proportion of lipids to plasmid DNA, morphology of the liposome, and the composition of the liposome are all important aspects of cellular nucleic acid transport. The physico-chemical features of liposomes that have been complexed with nucleic acids may differ from those of regular liposomes. The analysis was performed using dynamic light scattering (DLS) with liposomes (lipid : DOPE-1 : 1) and complexes (lipid : pDNA) at various N/P ratios of 1 : 1, 2 : 1, 4 : 1, and 8 : 1. The sizes of **C14-P**, **C14-M**, and **C14-S** liposomes were revealed to be 149 nm, 123 nm, and 122 nm, respectively, as shown in Fig. 2A. The sizes of the lipoplexes were observed increase dramatically from 164 nm to 384 nm, 131 nm to 358 nm, and 125 nm to 344 nm as the N/P ratio of lipid : pDNA complexes of **C14-P**, **C14-M**, and **C14-S** was extended from 1 : 1 to 8 : 1, respectively (Fig. 2C). The rise in the size with increasing N/P ratio could be explained by better subspaces at higher lipid contents. Furthermore, the maximum range of the size of the lipoplexes is 384 nm, demonstrating that they will be regarded to be optimal for effective gene transfections. The dicationic liposomes of **C14-P**, **C14-M**, and **C14-S** surface charges are +67, +73, and +74 mV, respectively (Fig. 2B). The surface potential of lipoplexes decreased compared to the corresponding liposomes when neutralized with pDNA (Fig. 2D). According to these findings, the proper size and surface potential of lipoplexes are necessary for successful transfection. Scanning electron microscopy was utilized to pictorially assess the DLS findings regarding the liposomal compositions. The visual images in Fig. 2E show that the liposomal particle sizes are substantially identical to the DLS results.

lipoplex, the proportion of lipids to plasmid DNA, morphology of the liposome, and the composition of the liposome are all important aspects of cellular nucleic acid transport. The physico-chemical features of liposomes that have been complexed with nucleic acids may differ from those of regular liposomes. The analysis was performed using dynamic light scattering (DLS) with liposomes (lipid : DOPE-1 : 1) and complexes (lipid : pDNA) at various N/P ratios of 1 : 1, 2 : 1, 4 : 1, and 8 : 1. The sizes of **C14-P**, **C14-M**, and **C14-S** liposomes were revealed to be 149 nm, 123 nm, and 122 nm, respectively, as shown in Fig. 2A. The sizes of the lipoplexes were observed increase dramatically from 164 nm to 384 nm, 131 nm to 358 nm, and 125 nm to 344 nm as the N/P ratio of lipid : pDNA complexes of **C14-P**, **C14-M**, and **C14-S** was extended from 1 : 1 to 8 : 1, respectively (Fig. 2C). The rise in the size with increasing N/P ratio could be explained by better subspaces at higher lipid contents. Furthermore, the maximum range of the size of the lipoplexes is 384 nm, demonstrating that they will be regarded to be optimal for effective gene transfections. The dicationic liposomes of **C14-P**, **C14-M**, and **C14-S** surface charges are +67, +73, and +74 mV, respectively (Fig. 2B). The surface potential of lipoplexes decreased compared to the corresponding liposomes when neutralized with pDNA (Fig. 2D). According to these findings, the proper size and surface potential of lipoplexes are necessary for successful transfection. Scanning electron microscopy was utilized to pictorially assess the DLS findings regarding the liposomal compositions. The visual images in Fig. 2E show that the liposomal particle sizes are substantially identical to the DLS results.

Heparin displacement experiments were also performed to substantiate the pDNA binding findings with the liposomal formulations mentioned above. Lipoplexes containing lipids **C14-P**, **C14-M**, and **C14-S** prevented the displacement of nucleic acid with heparin across the lipid : pDNA interface at N/P ratios 2 : 1–8 : 1 (Fig. 3B). These findings supported the previous report that amino acid head group-based cationic amphiphiles are stable over heparin.²¹

Lipoplexes were tested for serum resistance by incubating them in various concentrations of serum in DMEM medium. Gel electrophoresis was employed to track the flow of free DNA following incubation at a 2 : 1 N/P ratio, where the complete binding had happened. Surprisingly, even after incubation with 70% FBS in the medium, lipoplexes of **C14-P**, **C14-M**, and **C14-S** showed strong DNA binding. It has been determined that amino acid-based cationic lipids have acceptable serum resistance.³⁹ Whenever lipoplexes are delivered into the organism, this impact may aid in reducing payload leaking across the circulatory system.⁴⁰

2.5. Cytotoxicity study

Low cytotoxicity is another crucial trait that increases the likelihood of a synthetic nucleic acid delivery carrier being employed in medical chemistry. The MTT assay was used to determine the safety of the synthetic dicationic lipids under investigation. At lipid : pDNA N/P ratios of 1 : 1–8 : 1, the viability of **C14-P**/pDNA, **C14-M**/pDNA, and **C14-S**/pDNA complexes in HEK-293, CAL-27, and U87 cell lines was investigated. The cytotoxicity of cationic lipids is mostly determined by their positive charge potential.⁴¹ Synthesized dicationic lipids have a higher surface potential, not



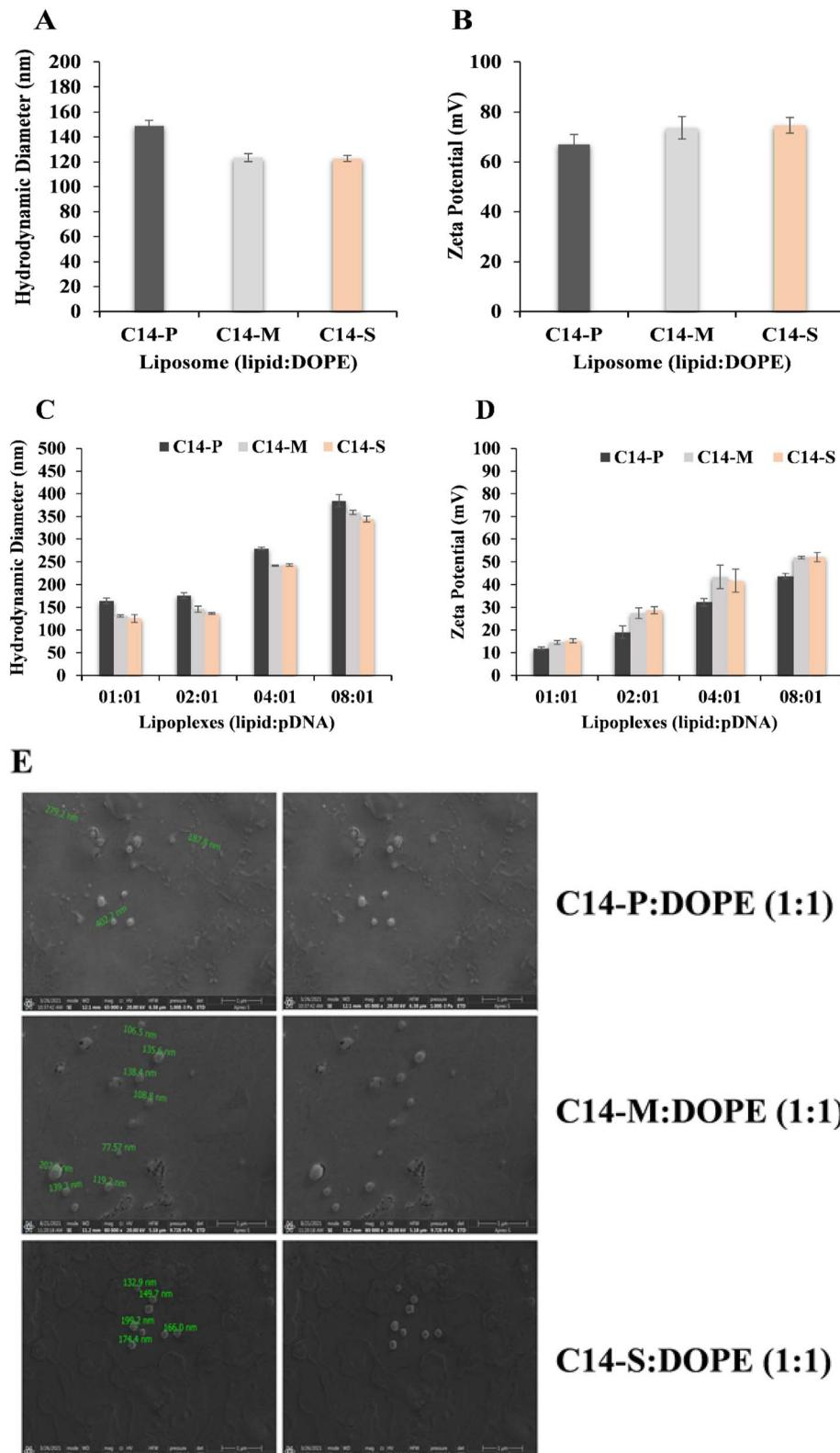


Fig. 2 Physicochemical characterizations: (A) hydrodynamic diameter; (B) zeta potentials of liposomal aggregates (lipid : DOPE-1 : 1); (C) hydrodynamic diameter (D) zeta potential of pDNA derived complexes 1 : 1 to 8 : 1 N/P ratio; (E) representative SEM images of transfection optimized liposomal formulation (lipid : DOPE-1 : 1).

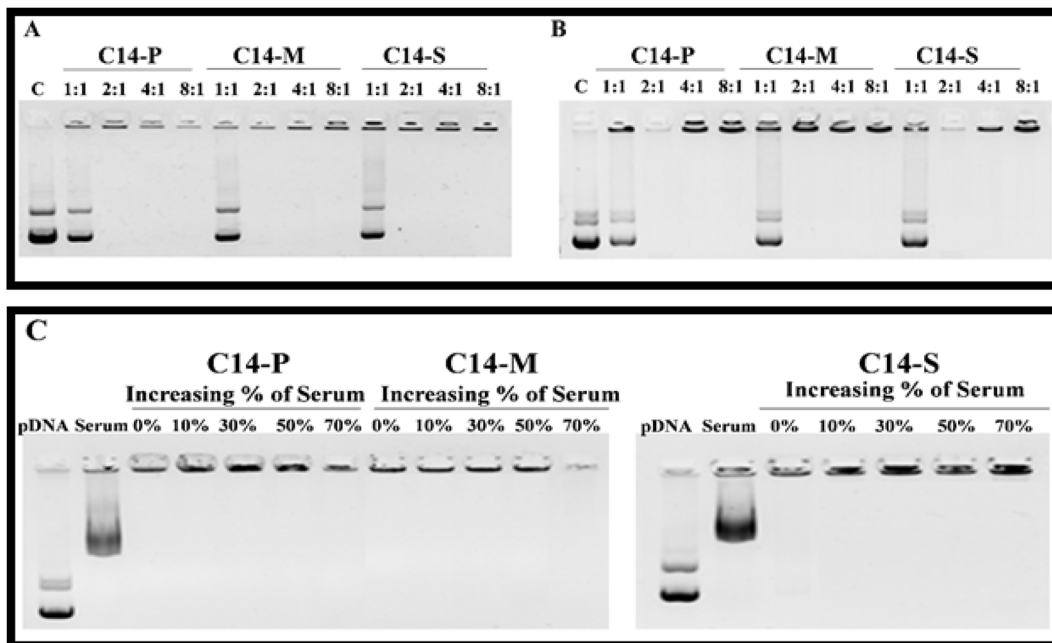


Fig. 3 C14-P, C14-M, and C14-S lipoplex-associated pDNA gel electrophoresis patterns in agarose gel retardation assay at 1:1–8:1 N/P ratio (A); heparin displacement analysis at 1:1–8:1 N/P ratio (B); serum stability of lipids at 0–70% at 2:1 N/P ratio (C); free pDNA and pDNA with serum are taken as control.

affecting cell viability. The compositions were discovered to have extraordinarily high cell viabilities (more than 85%), especially up to the lipid:pDNA N/P ratio 2:1 in comparison to the Lipofectamine-2000, which is observed. At higher N/P ratios of 4:1 and 8:1, cell viabilities of lipoplexes were reported to be 85–75% (Fig. 4A). These results revealed that lipid cytotoxicity does not appear to be a factor for differences in gene transfer efficacies. In all three cell lines tested, the C14-P, C14-M, and C14-S formulations were found to be less harmful. As a result, amino acid head group dicationic lipids are finer transfection reagents with reduced cytotoxicity, which is a significant property for *in vitro* and *in vivo* applications.

Natural amino acid-based cationic lipids could carry and transfect the therapeutic nucleic acid to the various cancerous cells.^{19,42} The current lipids tested for transfer of the anti-cancer gene, p53, into the glioma and oral cancer cells led to cell death. When these cells were treated with lipid/p53 lipoplexes, cell viability was dramatically less compared to lipid/pCMV- β -gal lipoplexes at a 2:1 N/P ratio (Fig. 4B). Moreover, in the case of C14-P, lipid cell death is more compared to C14-M and C14-S lipids in both U87 and CAL-27 cells. The visual images by optical microscope were recorded after 48 h of the transfection period of CAL-27 cells with lipid/pCMV- β -gal and lipid/p53 lipoplexes. Cell death is clearly recorded in the oral cancer cells for lipid/p53 lipoplexes (Fig. 4C). According to the revealed results, natural amino acid-based lipids typically carry the anticancer gene into cancer cells, leading to cell death.

2.6. Transfection biology

The transfection potentials of the lipids C14-P, C14-M, and C14-S were analyzed in three mammalian cultured cells (*i.e.*, HEK-

293, CAL-27, and U87). The reporter gene pCMV- β -gal, which encodes the enzyme β -galactosidase, was used to make lipoplexes of C14-P, C14-M, and C14-S lipids with lipid/pDNA N/P ratios ranging from 1:1 to 8:1. Despite the fact that the only structural variation between the lipids were the presence of proline, methionine, and serine head groups, C14-P was able to efficiently carry reporter gene into all three cell lines examined, especially when the N/P ratio is 2:1. Fig. 5 shows that lipoplexes of all three lipids enhanced transfection and displayed the highest percentage of protein production at 2:1 N/P ratio; this could be attributable to the smallest particle diameter and total binding of the pDNA, as well as the lowest cytotoxicity. More interestingly, the proline head group-based dicationic lipid (C14-P) has demonstrated superior transfection activity in all three cell lines, which is comparable to Lipofectamine-2000. The superior transfection efficacy of C14-P lipid may be due to the presence of a cyclic head group.^{43,44} Higher transfection efficiency of C14-P/DOPE vesicle indicates that proline-based cationic vectors have a great deal of ability as non-viral gene transfer vectors. The occurrence of cyclic head groups on the proline group of amino acid hybrid-transferring lipoplexes is, therefore, a crucial characteristic that can considerably alter the gene delivery efficacies of amino acid-based lipids, according to the comparative transfection patterns of C14-P.

In HEK-293 cells, qualitative and quantitative eGFP (enhanced green fluorescence protein) experiments were performed utilizing lipid/pEGFP mixtures at 4:1 and 2:1 N/P ratios to support the pCMV- β -gal reporter gene expression results. At this phase, it is crucial to determine whether pDNA expression (eGFP) reaches its maximum value at the chosen N/P ratio (4:1 and 2:1). An inverted microscope was used to



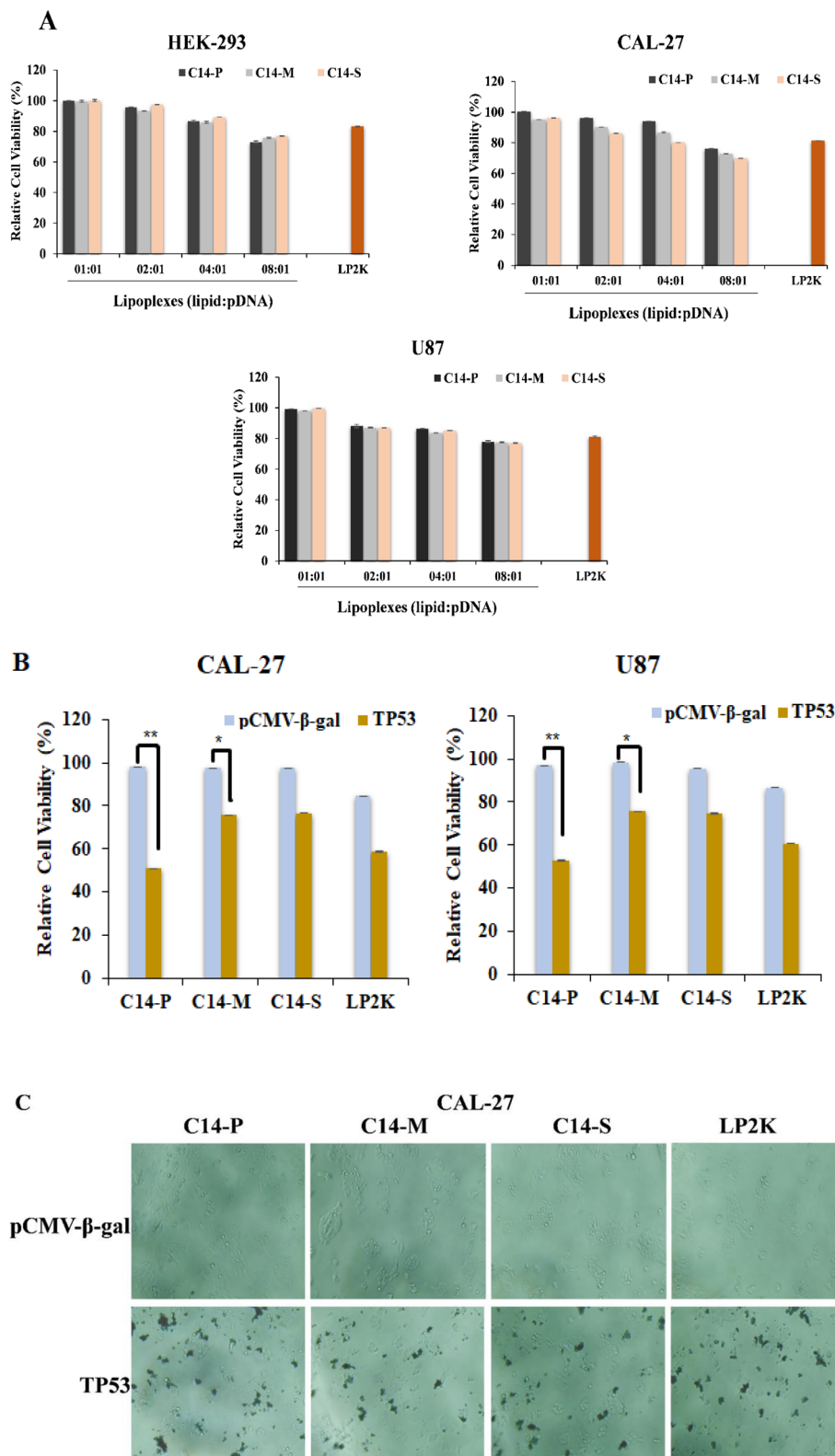


Fig. 4 Relative cell viabilities of lipids C14-P, C14-M, and C14-S in (A) HEK-293, CAL-27, and U87 cells using MTT assay; (B) cell viability of U87 and CAL-27 with lipid/pCMV-β-gal and lipid/p53 lipoplexes; (C) optical microscope images of CAL-27 cells after 48 h of incubation with lipid/pCMV-β-gal and lipid/p53 lipoplexes; statistical analysis: $n = 3$, $*P < 0.05$; $**P < 0.01$; $***P < 0.001$.

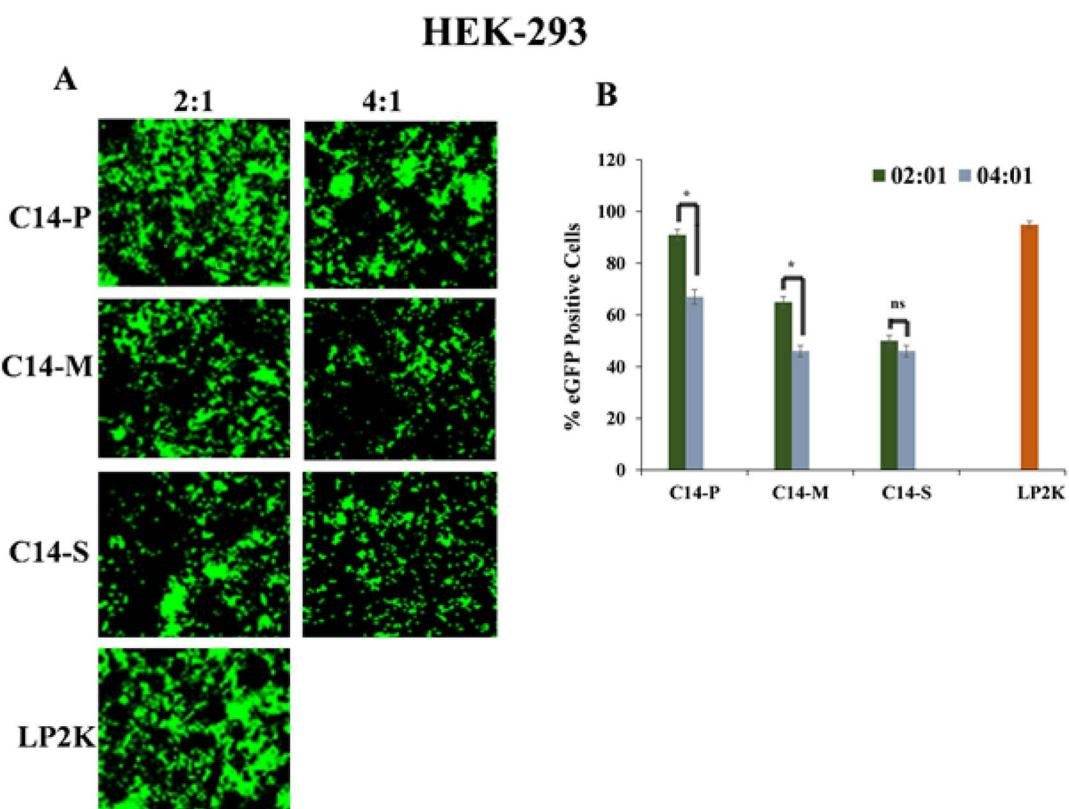
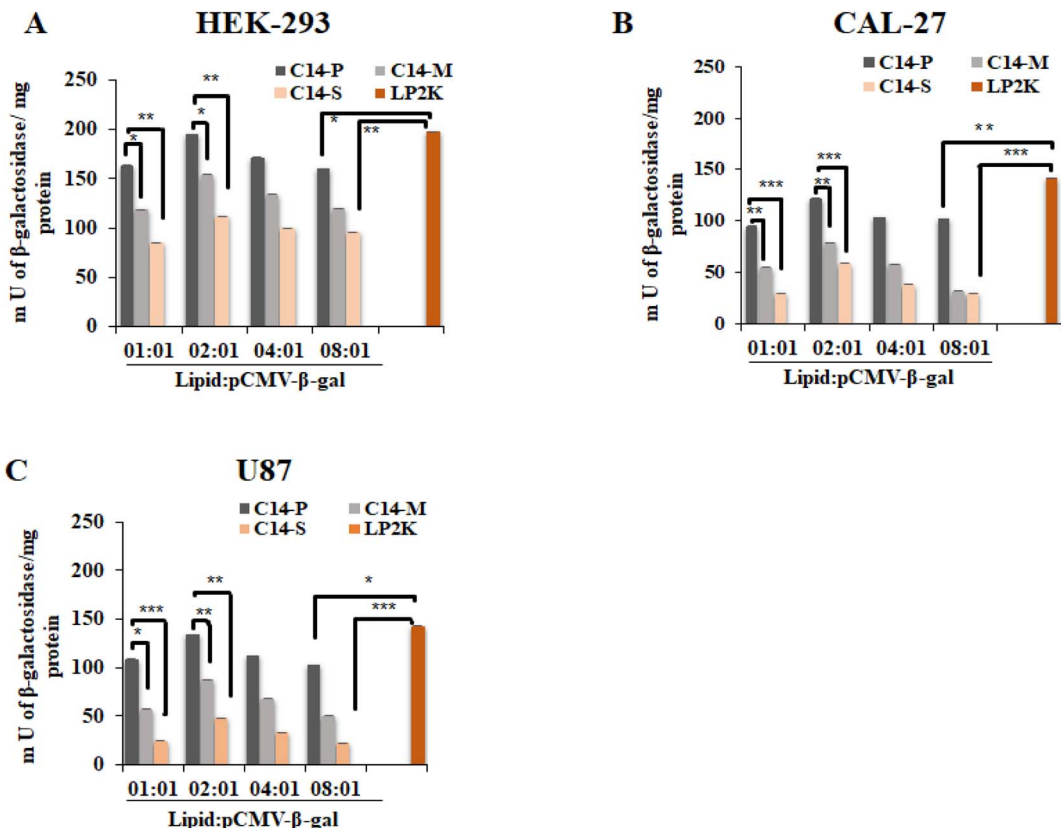


Fig. 6 (A) Green fluorescence expression of C14-P, C14-M, and C14-S lipoplexes (lipid/pEGFP) at 2:1 and 4:1 N/P ratios in HEK-293; (B) quantitative analysis of transfection potential in terms of percentage of eGFP positive cells. Statistical analysis: $n = 3$, * $P < 0.05$; ** $P < 0.01$; *** $P < 0.001$.



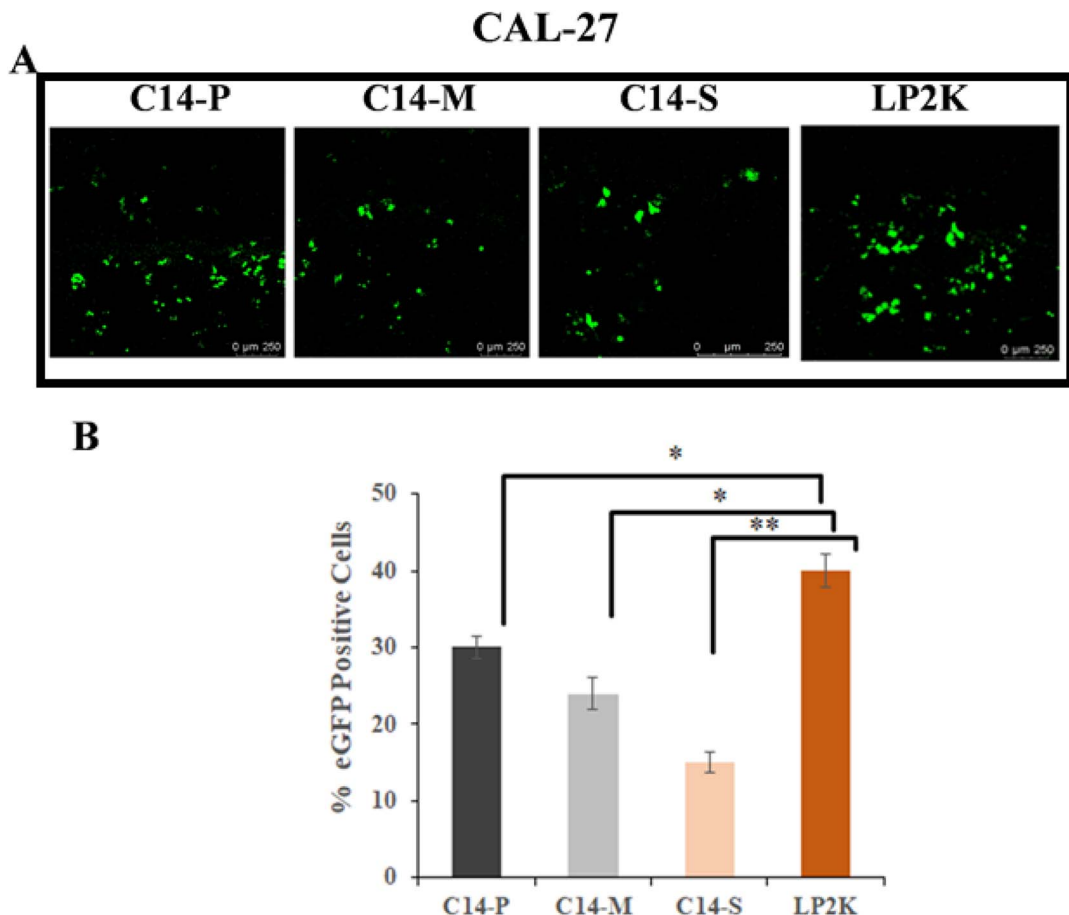


Fig. 7 (A) Green fluorescence images of C14-P, C14-M, and C14-S lipoplexes (lipid/pEGFP) at 2 : 1 N/P ratio in CAL-27; (B) quantitative analysis of transfection potential in terms of percentage of eGFP positive cells. Statistical analysis: $n = 3$, * $P < 0.05$; ** $P < 0.01$; *** $P < 0.001$.

examine the intracellular expression of eGFP. At the 4 : 1 and 2 : 1 N/P ratios, the percentage of eGFP expression in HEK-293 was found to be higher with **C14-P** and moderate with **C14-M** and **C14-S** (Fig. 6A). The percentage of positive eGFP cells of lipids were further confirmed by quantitative measurement of eGFP expression by flow cytometer, which was comparable to Lipofectamine-2000 (Fig. 6B). Further, eGFP expression was studied by qualitative and quantitative analysis in CAL-27 (Fig. 7A and B) and U87 (Fig. S25A and B†) cells at 2 : 1 N/P ratio. In both cell lines, **C14-P** has superior transfection compared to **C14-M** and **C14-S**. According to the transfection outcomes, it could be inferred that the proline head group on a hydrophobic long chain-based lipid is an effective method for gene delivery.

2.7. Intracellular uptake

Transfection results demonstrated that **C14-P**, **C14-M**, and **C14-S** lipids exhibited higher transfection efficiency in all three cell lines (HEK-293, CAL-27, and U87) when the lipid/pDNA N/P ratio was 2 : 1; moreover, C14 lipid showed superior expression. HEK-293 and CAL-27 cells were tested with lipoplexes containing pCMV- β -gal and rhodamine-PE labelled liposomes of **C14-P**, **C14-M**, and **C14-S** spanning the lipid/pDNA N/P ratio of 2 : 1 to check

whether the highest absorption occurs with **C14-P** lipid. DAPI (4',6-diamidino-2-phenylindole) was utilized to stain the cell nucleus. Cellular uptake of rhodamine-PE tagged lipoplexes in CAL-27 (Fig. 8A and B) and HEK-293 cells (Fig. S26A and B†) were examined, and the results indicated that **C14-P** lipid had higher intracellular uptake compared to **C14-M** and **C14-S** lipids. These results corroborated the transfection results and revealed that among the three synthesized cationic lipids, proline-based lipids have the superior capability in *in vitro* gene delivery.

2.8. Conclusions

The current study demonstrates the design, synthesis, physicochemical properties, and respective *in vitro* transfection efficiencies of cationic lipids (*i.e.* **C14-P**, **C14-M**, and **C14-S**) tested against three cell lines. Cytotoxicity of the cationic lipids in three different cell lines was found to be minimal. Furthermore, the green fluorescence and β -galactosidase activity investigations support the findings of the *in vitro* transfection. Lipoplexes of **C14-P**, **C14-M**, and **C14-S** lipids are compared in terms of serum stability, cytotoxicity, transfection efficiency, and cellular absorption. According to the results, **C14-P** is a promising nanovesicle as a reliable transfection reagent for a primary cultured cell line with relatively low cytotoxicity.



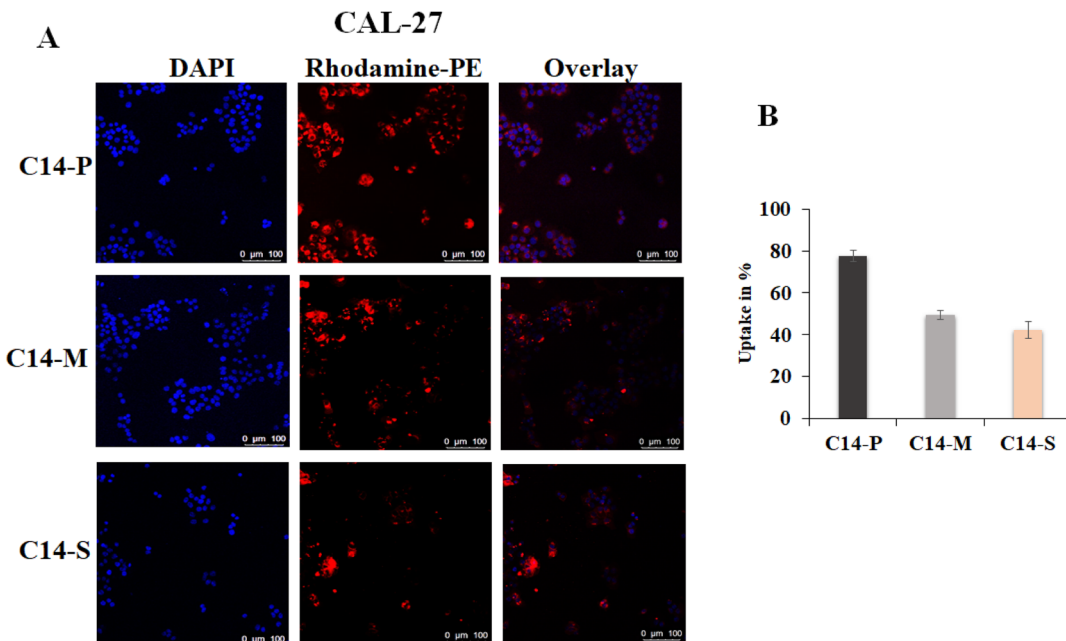


Fig. 8 (A) Qualitative uptake images (B) quantitative uptake percentage of CAL-27 cells transfected with rhodamine-labelled lipoplexes of lipids C14-P, C14-M, and C14-S prepared at higher transfection lipid/pDNA N/P ratio 2 : 1; nucleus (DAPI), and cytoplasm (Rh-PE).

3. Experimental section

3.1. Materials

Fmoc-amino acids, *p*-toluene sulfonic acid, dicyclohexylcarbodiimide (DCC), 4-dimethylaminopyridine, and 1-bromo tetradecane were delivered from Sigma Aldrich. The organic solvents and chemicals, including ethanolamine, potassium carbonate, piperidine, dimethylformamide (DMF), methylene dichloride (DCM), and ethyl acetate, were purchased from Spectrochem Pvt. Ltd., and Finar Limited. Molecular mass analyses were performed by High-Resolution Mass Spectrometry (HRMS) using Agilent Q-TOF 6230, and the purity of final lipids was characterized by HPLC (Shimadzu LC Solution). ¹H-NMR (400 MHz) and ¹³C-NMR (101 MHz) spectra were recorded on Bruker AVANCE spectrometer, with TMS as an internal standard. DOPE (1,2-dioleoyl-*sn*-glycerol-3-phosphoethanolamine) was purchased from Sigma Aldrich. Agarose and 6× loading dye were purchased from Hi-media, India. All chemicals for biological applications were procured from Merck, Sigma-Aldrich, Thermo Fischer Scientific, and Invitrogen.

3.2. Synthesis

3.2.1 Synthesis of 2-(di-tetradecylamino)-ethanol ((C14)₂NEOH). 4.0 g (65.48 mmol) of ethanolamine, 20 mL of ethyl acetate, and 9.05 g (65.48 mmol) of potassium carbonate were combined in a 100 mL RB flask. This combined mixture was maintained at 60 °C and 39.99 g (130.96 mmol) of 1-bromo tetradecane was applied after 15 min of stirring and the reaction began overnight. After consumption of starting components, the mixture was allowed to refrigerate to room temperature, and the solvent was removed, subjecting it to rotary evaporation. The resulting crude was dissolved in excess ethyl acetate (200

mL), washed three times (3 × 100 mL) with normal drinking water and once with brine solution (50 mL). Subsequently, the organic layer was separated, dried with anhydrous sodium sulphate to remove the remaining water content, and the solvent was evaporated under vacuum pressure. The resulting residue was chromatographically filtered using 1% EtOAc/PE as the eluent to 60–120 mesh size silica gel board. Yield: 3.46 g (6.79 mmol, 86.50%) strong white oily; ¹H NMR (CDCl₃) [δ/ ppm] 3.52 (t, *J* = 5.2 Hz, 2H), 2.56 (t, *J* = 5.2 Hz, 2H), 2.45 (t, *J* = 7.6 Hz, 4H), 1.42 (s, 4H), 1.26 (s, 46H), 0.88 (t, *J* = 6.6 Hz, 6H); ¹³C{¹H} NMR (CDCl₃) [δ/ ppm] 58.34, 55.52, 53.84, 31.94, 29.67, 29.61, 29.38, 27.46, 27.19, 22.70, 14.12; MS *m/z*: 453.4910, found: 454.4983[M + H]⁺.

3.2.2 Synthesis of 2-(di-tetradecylamino)-ethyl (Fmoc)-amino acid (1a, 2a, 3a). DCC (5.47 mmol), *p*-toluene sulfonic acid (5.46 mmol) and 2-(di-tetradecylamino)-ethanol (4.56 mmol) were applied to the stirred solution of Fmoc-amino acid (4.58 mmol), a catalytic amount of 4-dimethylaminopyridine, and 5 mL of dry DCM, and the mixture of components was stirred at RT until the starting components were completely processed. Once the reaction mixture was removed from stirring, it was dissolved in ethyl acetate solvent (100 mL) and washed with excess normal drinking water (3 × 80 mL). Then, the product layer was separated from the water layer and dried with anhydrous Na₂SO₄ to eliminate traces of residual water, followed by evaporation of the solvent at reduced pressure. The product demonstrating the *R*_f in the 9 : 1 PE and EtOAc range 0.5–0.7 was purified using 1% ethyl acetate in pet ether eluent column chromatography.

3.2.2.1 2-(Di-tetradecylamino)-ethyl (Fmoc)-proline (1a). Product: pale white solid, 1.59 mmol (1.23 g), yield: 82%; ¹H NMR (CDCl₃) [δ/ ppm] 7.75 (t, *J* = 6.0 Hz, 2H), 7.59 (m, 2H), 7.39



(dd, $J = 14.4, 7.6$ Hz, 2H), 7.31 (dd, $J = 7.6, 3.6$ Hz, 2H), 4.41 (d, $J = 7.2$ Hz, 2H), 4.34 (t, $J = 5.2$ Hz, 1H), 4.31–4.25 (m, 1H), 4.22–4.09 (m, 2H), 3.67 (d, $J = 7.6$ Hz, 1H), 3.54 (d, $J = 7.6$ Hz, 1H), 2.64 (s, 2H), 2.39 (t, $J = 6.8$ Hz, 2H), 2.29 (t, $J = 8.0$ Hz, 2H), 2.04 (t, $J = 7.6$ Hz, 2H), 2.00–1.85 (m, 2H), 1.68–1.16 (m, 46H), 0.88 (t, $J = 6.8$ Hz, 6H); $^{13}\text{C}\{\text{H}\}$ NMR (CDCl₃) [δ/ppm] 169.49, 154.58, 141.63, 139.06, 127.98, 127.60, 127.21, 126.67, 125.53, 124.36, 124.00, 120.59, 119.93, 63.08, 61.31, 60.55, 57.81, 55.94, 54.20, 53.81, 46.35, 46.23, 38.70, 31.93, 29.70, 29.68, 29.66, 29.61, 29.59, 29.45, 29.37, 27.26, 25.92, 24.88, 24.07, 22.70, 14.13; MS *m/z*: 772.6118, found: 773.6208 [M + H]⁺.

3.2.2.2 2-(Di-tetradecylamino)-ethyl (Fmoc)-methionine (2a). Product: pale white solid, 1.47 mmol (1.19 g), yield: 79%; ^1H NMR (CDCl₃) [δ/ppm] 7.68 (d, $J = 7.6$ Hz, 2H), 7.52 (d, $J = 7.2$ Hz, 2H), 7.31 (t, $J = 7.4$ Hz, 2H), 7.23 (t, $J = 7.6$ Hz, 2H), 4.42 (d, $J = 4.4$ Hz, 1H), 4.34 (d, $J = 7.2$ Hz, 2H), 4.14 (t, $J = 7.0$ Hz, 2H), 4.06–4.01 (m, 1H), 2.62 (t, $J = 6.0$ Hz, 2H), 2.46 (t, $J = 7.2$ Hz, 2H), 2.36 (t, $J = 7.2$ Hz, 2H), 2.01 (s, 3H), 1.95 (s, 2H), 1.50–1.09 (m, 48H), 0.80 (m, 6H); $^{13}\text{C}\{\text{H}\}$ NMR (CDCl₃) [δ/ppm] 168.62, 158.16, 141.33, 140.40, 135.19, 129.36, 129.03, 127.36, 125.32, 124.27, 121.29, 120.91, 120.66, 119.94, 61.64, 58.21, 55.82, 53.92, 46.13, 32.91, 31.82, 29.57, 29.54, 29.24, 27.14, 25.94, 25.89, 22.60, 14.25; MS *m/z*: 806.5995, found: 807.6127 [M + H]⁺.

3.2.2.3 2-(Di-tetradecylamino)-ethyl (Fmoc)-serine (3a). Product: pale white solid, 1.75 mmol (1.34 g), yield: 89.33%; ^1H NMR (CDCl₃) [δ/ppm] 7.65 (d, $J = 7.2$ Hz, 2H), 7.61 (d, $J = 7.6$ Hz, 2H), 7.33–7.27 (m, 2H), 7.24–7.20 (m, 2H), 4.40 (d, $J = 6.0$ Hz, 2H), 4.03 (t, $J = 6.2$ Hz, 1H), 3.97 (t, $J = 6.8$ Hz, 1H), 3.55 (t, $J = 6.4$ Hz, 2H), 2.61 (t, $J = 6.2$ Hz, 2H), 2.38 (t, $J = 7.4$ Hz, 4H), 1.96 (d, $J = 3.2$ Hz, 2H), 1.20 (m, 48H), 0.80 (t, $J = 6.8$ Hz, 6H); $^{13}\text{C}\{\text{H}\}$ NMR (CDCl₃) [δ/ppm] 166.04, 155.83, 145.87, 141.58, 126.67, 125.53, 124.32, 124.00, 121.01, 120.59, 119.93, 119.82, 119.74, 63.08, 61.31, 57.81, 54.20, 53.81, 46.35, 31.93, 29.70, 29.68, 29.61, 29.59, 29.45, 29.37, 27.26, 25.92, 24.07, 22.70, 14.13; MS *m/z*: 762.5911, found: 763.6040 [M + H]⁺.

3.2.3 Synthesis of 2-(di-tetradecylamino)-ethyl amino acid and final lipids. Intermediate 1a or 2a or 3a (1.29 mmol) was kept in a 100 mL RB flask, inserted 5 mL DMF with 20% piperidine, and stirred overnight. Then, the reaction mixture was dissolved in 150 mL ethyl acetate solvent and then washed twice with an excess of cold drinking water. Using sodium sulphate, the organic layer was dried and the solvent evaporated on a rotary evaporator. The crude indicating *R*_f 0.4 in 9 : 1 PE/EtOAc was filtered by a column using 60–120 mesh size silica gel and eluted with 3% EtOAc/PE. The obtained Fmoc deprotected amino acid compounds quaternized with 6 N HCl under reflux conditions yielded the final lipid.

3.2.3.1 2-(Di-tetradecylamino)-ethyl proline (C14-P). Product: light yellow solid oily, yield: 0.82 g (1.48 mmol), 82%; ^1H NMR (CDCl₃) [δ/ppm] 4.09 (ddd, $J = 20.8, 8.4, 3.8$ Hz, 1H), 3.80 (t, $J = 4.8$ Hz, 2H), 3.46 (d, $J = 5.0$ Hz, 1H), 3.36 (d, $J = 10.4$ Hz, 1H), 2.98 (t, $J = 4.8$ Hz, 2H), 2.90 (dd, $J = 5.0$ Hz, 2H), 2.10 (d, $J = 7.8$ Hz, 1H), 1.91 (d, $J = 12.4$ Hz, 1H), 1.74 (t, $J = 5.2$ Hz, 2H), 1.59 (s, 2H), 1.36–1.12 (m, 48H), 0.81 (t, $J = 6.9$ Hz, 6H); $^{13}\text{C}\{\text{H}\}$ NMR (CDCl₃) [δ/ppm] 170.94, 62.21, 54.96, 53.20, 52.64, 31.92, 29.70, 29.66, 29.62, 29.53, 29.48, 29.36, 29.18, 27.36, 27.18, 27.01, 22.68, 21.02, 14.11; MS *m/z*: 552.5583, found: 552.5521 [M]⁺.

3.2.3.2 2-(Di-tetradecylamino)-ethyl methionine (C14-M). Product: light yellow solid oily, yield: 0.85 g (1.45 mmol), 85%; ^1H NMR (CDCl₃) [δ/ppm] 4.52 (t, $J = 4.0$ Hz, 2H), 4.10 (t, $J = 6.4$ Hz, 1H), 2.62 (t, $J = 6.0$ Hz, 2H), 2.55 (m, 2H), 2.43 (t, $J = 7.6$ Hz, 2H), 2.36 (t, $J = 7.6$ Hz, 2H), 2.03 (s, 3H), 2.02–1.93 (m, 2H), 1.43–1.18 (m, 48H), 0.81 (t, $J = 6.4$ Hz, 6H); $^{13}\text{C}\{\text{H}\}$ NMR (CDCl₃) [δ/ppm] 174.96, 61.71, 56.58, 56.35, 56.15, 53.67, 31.90, 29.68, 29.66, 29.64, 29.62, 29.58, 29.51, 29.48, 29.44, 29.40, 29.34, 29.07, 26.72, 22.66, 20.79, 14.08; MS *m/z*: 586.5460, found: 586.5440 [M]⁺.

3.2.3.3 2-(Di-tetradecylamino)-ethyl serine (C14-S). Product: light yellow solid oily, yield: 0.81 g (1.49 mmol), 81%; ^1H NMR (CDCl₃) [δ/ppm] 4.31 (t, $J = 4.0$ Hz, 2H), 4.02 (s, 1H), 3.64 (t, $J = 4.8$ Hz, 2H), 3.50–3.46 (m, 1H), 3.33–3.28 (m, 1H), 2.71 (t, $J = 4.8$ Hz, 2H), 2.60 (t, $J = 7.6$ Hz, 4H), 1.27 (d, $J = 10.0$ Hz, 48H), 0.87 (t, $J = 6.4$ Hz, 6H); $^{13}\text{C}\{\text{H}\}$ NMR (CDCl₃) [δ/ppm] 172.63, 62.30, 60.07, 50.58, 49.72, 31.91, 29.69, 29.52, 29.33, 28.86, 26.77, 22.68, 21.37, 14.10; MS *m/z*: 542.5375, found: 542.5335 [M]⁺.

3.3. Preparation of liposomes

In an autoclaved dry glass vial, the cationic lipid and the supplementary lipid (DOPE) were both dissolved in dry chloroform (1 : 1 mM concentration). The chloroform was evaporated using a thin stream of nitrogen gas, and then the thin film was dried for 5 h under vacuum. The dried lipid film was then swollen for 12 h with 1 mL Milli Q water. After that, the sample was vortexed at ambient temperature for 2–3 min for a clear solution and then kept for sonication in a bath sonicator to form multilamellar vesicles (MLVs). Subsequently, MLVs were sonicated in a cool bath until they were clear, using a Branson Sonifier with a 25 W output voltage. The obtained clear aqueous liposomes were used for lipoplex formation.

3.4. Zeta potential (mV) and size (nm) measurements

Zeta sizer 3000HSA equipped using a diode-pumped solid-state laser at 532 nm set at 25 °C was used to quantify the sizes of lipid aggregates and the resultant complexes from the plasmid. From freshly produced liposomes (1 : 1 charge ratio), 100 μL were diluted to 900 μL of Milli-Q in quartz cuvette prior to the measurements. Each co-liposomal formulation was used to make lipoplexes with 5 μL (100 ng μL^{-1}) of pDNA (pCMV-β-gal), 30 min before measurement at 1 : 1, 2 : 1, 4 : 1, and 8 : 1 N/P ratios. Milli-Q water was used to dilute the samples to 1000 μL of the final volume before analysis. The average value of three different measures taken in general mode with the software of a Zeta sizer 3000HSA (Malvern, UK) was taken into consideration. The surface charges of lipoplexes with pCMV-β-gal were measured at a fixed angle of 93° using the same instrument with a different zeta cuvette. Each sample value was taken as the proportion of three different readings.

3.5 Scanning electron microscopy (SEM)

A glass slide was applied with 10 μL of liposome, which was placed on a Cu grid with a carbon layer. Using a fresh filter paper, the excess stain was removed and dried at air pressure at room



temperature before being examined with an FEI (Apreo LoVac) scanning electron microscope on Mn- $k\alpha$ at a resolution of 127 eV.

3.6. Agarose gel electrophoresis

One of the most useful assays for visually predicting the exact pDNA binding capabilities of lipid solutions is gel electrophoresis. Lipoplexes were made by combining 5 μ L of supercoiled pDNA (100 ng μ L $^{-1}$) with various amounts of lipid concentrations in a total volume of 24 μ L, with the final lipid : pDNA N/P ratios, 1 : 1 to 8 : 1, in a typical experiment. After 30 min of incubation, each lipoplex solution (12 μ L) was placed into 1% agarose gel (pre-stained with ethidium bromide) and electrophoresis was performed (100 V, 35 min). The Bio-Rad Gel Doc imaging equipment was used to visualize the bands.

3.7. Heparin displacement assay

The lipid : pDNA complexes were produced and incubated for 30 min as described above (agarose gel electrophoresis). These lipid : pDNA complexes were then incubated with heparin sodium salt (0.1 μ g) for another 30 min. For heparin displacement analysis, the samples were subjected to electrophoresis in a 1% agarose gel.

3.8. Serum stability

For serum stability assay, each lipid lipoplexes prepared at 2 : 1 N/P ratio for five concentrations of serum and incubated for 30 minutes. These lipoplex solutions were added to FBS in DMEM medium at 10–70% of serum concentrations. Then, these complexes were again incubated for 2 h, before subjecting to gel electrophoresis. The gel electrophoresis was conducted at 100 V for 35 min.

3.9. Cells & cell culture

The National Centre for Cell Sciences provided CAL-27 (oral adenosquamous cell carcinoma), HEK-293 (human embryonic kidney) and U87 (human primary glioblastoma) cells (Pune, India). Mycoplasma was not found in any of the cells. The cells were grown in DMEM (Dulbecco's Modified Eagle's Medium) containing 10% fetal bovine serum (FBS). All studies were conducted using cultures that were 85–90% confluent. For cell viability and transfection studies, cell lines were trypsinized, counted, and sub-cultured into 96-well, 24-well, and 12-well plates. Before being utilized in tests, the cells were allowed to adhere for 20–24 h.

Conflicts of interest

There are no conflicts to declare.

Acknowledgements

SM express gratitude to NIT Warangal, India, for a research fellowship. Dr Srilakshmi V. Patri is grateful to SERB, Department of Science & Technology (DST), Government of India, New Delhi, for financial support (CRG/2018/001049).

References

- I. M. Verma and N. Somia, *Nature*, 1997, **387**, 239–242.
- B. A. Bunnell and R. A. Morgan, *Clin. Microbiol. Rev.*, 1998, **11**, 42–56.
- S. Ylä-Herttuala and J. F. Martin, *Lancet*, 2000, **355**, 213–222.
- M. R. Knowles, K. W. Hohneker, Z. Zhou, J. C. Olsen, T. L. Noah, P.-C. Hu, M. W. Leigh, J. F. Engelhardt, L. J. Edwards, K. R. Jones, M. Grossman, J. M. Wilson, L. G. Johnson and R. C. Boucher, *N. Engl. J. Med.*, 1995, **333**, 823–831.
- Y. Yang, F. A. Nunes, K. Berencsi, E. Gönczöl, J. F. Engelhardt and J. M. Wilson, *Nat. Genet.*, 1994, **7**, 362–369.
- C. McGregor, C. Perrin, M. Monck, P. Camilleri and A. J. Kirby, *J. Am. Chem. Soc.*, 2001, **123**, 6215–6220.
- B. Kedika and S. V. Patri, *Eur. J. Med. Chem.*, 2014, **74**, 703–716.
- V. Muripiti, B. Lohchania, V. Ravula, S. Manturthi, S. Marepally, A. Veliandhi and S. V. Patri, *New J. Chem.*, 2021, **45**, 615–627.
- D. M. Lynn, D. G. Anderson, D. Putnam and R. Langer, *J. Am. Chem. Soc.*, 2001, **123**, 8155–8156.
- M. X. Tang, C. T. Redemann and F. C. Szoka, *Bioconjugate Chem.*, 1996, **7**, 703–714.
- Y. Lee, H. Koo, Y. B. Lim, Y. Lee, H. Mo and J. S. Park, *Bioorg. Med. Chem. Lett.*, 2004, **14**, 2637–2641.
- D. Niculescu-Duvaz, J. Heyes and C. Springer, *Curr. Med. Chem.*, 2005, **10**, 1233–1261.
- K. Ewert, A. Ahmad, H. M. Evans, H. W. Schmidt and C. R. Safinya, *J. Med. Chem.*, 2002, **45**, 5023–5029.
- M. Gosangi, H. Rapaka, V. Ravula and S. V. Patri, *Bioconjugate Chem.*, 2017, **28**, 1965–1977.
- B. Kedika and S. V. Patri, *J. Med. Chem.*, 2011, **54**, 548–561.
- D. Lechardeur and G. L. Lukacs, *Curr. Gene Ther.*, 2002, **2**, 183–194.
- I. S. Zuhorn and D. Hoekstra, *J. Membr. Biol.*, 2002, **189**, 167–179.
- Y. Xu and F. C. Szoka, *Biochemistry*, 1996, **35**, 5616–5623.
- V. Ravula, Y. L. Lo, Y. T. Wu, C. W. Chang, S. V. Patri and L. F. Wang, *Mater. Sci. Eng., C*, 2021, **126**, 112189.
- B. Kedika and S. V. Patri, *Mol. Pharm.*, 2012, **9**, 1146–1162.
- H. Rapaka, S. Manturthi, P. Arjunan, V. Venkatesan, S. Thangavel, S. Marepally and S. V. Patri, *ACS Appl. Bio Mater.*, 2022, **5**, 1489–1500.
- M. Gosangi, T. Y. Mujahid, V. Gopal and S. V. Patri, *Org. Biomol. Chem.*, 2016, **14**, 6857–6870.
- V. Muripiti, B. Lohchania, S. K. Marepally and S. V. Patri, *Medchemcomm*, 2018, **9**, 264–274.
- V. Ravula, V. Muripiti, S. Manthurthi and S. V. Patri, *ChemistrySelect*, 2021, **6**, 13025–13033.
- J. Sen and A. Chaudhuri, *Bioconjugate Chem.*, 2005, **16**, 903–912.
- P. P. Karmali, V. V. Kumar and A. Chaudhuri, *J. Med. Chem.*, 2004, **47**, 2123–2132.
- J. Wang, X. Guo, Y. Xu, L. Barron and F. C. Szoka, *Society*, 1998, **2623**, 2207–2215.
- S.-J. Lee and C.-H. Ahn, *Macromol. Res.*, 2006, **14**, 129–131.



29 S. Pujals and E. Giralt, *Adv. Drug Delivery Rev.*, 2008, **60**, 473–484.

30 A. M. Cardoso, C. M. Morais, A. R. Cruz, S. G. Silva, M. L. Do Vale, E. F. Marques, M. C. P. De Lima and A. S. Jurado, *Eur. J. Pharm. Biopharm.*, 2015, **89**, 347–356.

31 S. L. Borrego, J. Fahrmann, J. Hou, D. W. Lin, B. J. Tromberg, O. Fiehn and P. Kaiser, *J. Lipid Res.*, 2021, **62**, 100056.

32 P. Kaiser, *Biomolecules*, 2020, **10**, 7–9.

33 V. Ravula, Y.-L. Lo, Y.-T. Wu, C.-W. Chang, S. V. Patri and L.-F. Wang, *Mater. Sci. Eng., C*, 2021, **126**, 112189.

34 E. Yonish-Rouach, D. Resnftzky, J. Lotem, L. Sachs, A. Kimchi and M. Oren, *Nature*, 1991, **352**, 345–347.

35 R. W. Johnstone, A. A. Ruefli and S. W. Lowe, *Cell*, 2002, **108**, 153–164.

36 G. Shim, M. G. Kim, J. Y. Park and Y. K. Oh, *Asian J. Pharm. Sci.*, 2013, **8**, 72–80.

37 H. Elsana, T. O. B. Olusanya, J. Carr-wilkinson, S. Darby, A. Faheem and A. A. Elkordy, *Sci. Rep.*, 2019, **9**, 1–17.

38 M. Gosangi, H. Rapaka, T. Y. Mujahid and S. V. Patri, *Medchemcomm*, 2017, **8**, 989–999.

39 L. Li, H. Song, K. Luo, B. He, Y. Nie, Y. Yang, Y. Wu and Z. Gu, *Int. J. Pharm.*, 2011, **408**, 183–190.

40 M. M. Mady and M. M. Ghannam, *Afr. J. Pharm. Pharmacol.*, 2011, **5**, 1898–1905.

41 G. Smistad, J. Jacobsen and S. A. Sande, *Int. J. Pharm.*, 2007, **330**, 14–22.

42 V. Ravula, Y. L. Lo, L. F. Wang and S. V. Patri, *ACS Omega*, 2021, **6**, 22955–22968.

43 B. K. Majeti, R. S. Singh, S. K. Yadav, S. R. Bathula, S. Ramakrishna, P. V. Diwan, S. S. Madhavendra and A. Chaudhuri, *Chem. Biol.*, 2004, **11**, 427–437.

44 H. Gao and K. M. Hui, *Gene Ther.*, 2001, **8**, 855–863.

